Unusual Structural Properties of Switchback DNA

Bharath Raj Madhanagopal,[1] Hannah Talbot,[1] Arlin Rodriguez,[1] Jiss Maria Louis,[1] Hana Zeghal,[1] Sweta Vangaveti,[1] Kaalak Reddy,[1,2] and Arun Richard Chandrasekaran[1]*

[1]The RNA Institute, University at Albany, State University of New York, Albany, NY, USA.

[2]Department of Biological Sciences, University at Albany, State University of New York, Albany, NY, USA.

*Correspondence: arun@albany.edu

Abstract

Synthetic DNA motifs form the basis of nucleic acid nanotechnology, and their biochemical and biophysical properties determine their applications. Here, we present a detailed characterization of switchback DNA, a globally left-handed structure composed of two parallel DNA strands. Compared to a conventional duplex, switchback DNA shows lower thermodynamic stability and requires higher magnesium concentration for assembly, but exhibits a higher biostability against some nucleases. Strand competition and strand displacement experiments show that component sequences have an absolute preference for duplex complements instead of their switchback partners. Further, we hypothesize a potential role for switchback DNA as an alternate structure for short-tandem repeats involved in repeat-expansion diseases. Together with small molecule binding experiments and cell studies, our results open new avenues for synthetic DNA motifs in biology and nanotechnology.

Molecular self-assembly using DNA allows the intricate design of nanostructures with custom shapes and sizes, programmable features and site-specific functionalization.[1] DNA motifs such as the double crossover (DX),[2] triple crossover (TX),[3] paranemic crossover (PX),[4] and multi-arm DNA stars[5,6] are structural units used to produce various finite[7–9] and extended assemblies.[5,10,11] Characterization of DNA motifs and understanding their properties has contributed to the development of design principles and expansion of the DNA nanotechnology toolset to create nanometer- to micrometer-scale static structures[12,13] and dynamic devices.[14,15] To integrate a DNA motif as a structural unit in DNA nanostructures, several factors are considered: geometric parameters of the motif, thermal stability, structural robustness, polarity of the strands and the helical handedness. Chemical functionalization and design-based strategies yield nanostructures that are thermally stable[16] and nuclease-resistant.[17] Identical terminal polarities in a double helical context are typically achieved through specific sequence choices, DNA analogs or pH control to form parallel stranded DNA[18,19] and by the incorporation of 3′-3′ or 5′-5′ linkages that leaves two 5′ ends or 3′ ends on the DNA motifs respectively.[20] To introduce left-handed helices, Z-DNA forming sequences[21] or L-DNA component strands[22] are typically incorporated into component DNA strands. Detailed study of underlying DNA structures and new DNA motifs informs on the rational design of functional characteristics in self-assembled nanostructures.

In this work, we present a detailed characterization and hypothesize a potential biological relevance of a DNA motif called the switchback DNA, first suggested by Seeman[4] and later reported as an artificial left-handed structure by Mao.[23] Although the motif and its self-assembly into a lattice was recently reported,[24] the biochemical and biophysical properties of this molecule is unknown. The impact of its unusual left-handed topology and parallel strand orientation on the physico-chemical properties of the motif is of potential interest in DNA nanotechnology and nucleic acid structure in general. Here, we compared switchback DNA with a conventional B-form duplex using biochemical and biophysical techniques. We analyzed small molecule binding in the two structures, aided by molecular docking and studied the relative biostability of switchback DNA against five different nucleases. Moreover, we hypothesize that switchback DNA has the propensity to form as a biologically relevant alternate DNA structure within short tandem repeats that are involved in several repeat-expansion diseases. Our study provides a deeper understanding of the properties of switchback DNA, its potential role in biology and prospects in DNA nanotechnology.

Assembly and characterization of switchback DNA

The switchback DNA motif is assembled from two DNA strands and contains a series of B-DNA half-turns aligned laterally (**Fig. 1a**).[23,24] The structure shown in **Fig. 1a** contains two half-turns, where the helical axis of the half-turn domains is perpendicular to the axis of the full structure. Each half-turn domain consists of six base pairs, with the gray and red strands in **Fig. 1a** being complementary in the switchback sense. We

use the term "switchback complement" for a strand that can form a switchback structure with another strand, and the term "duplex complement" for a strand that forms a conventional B-form duplex (eg: gray and blue strands in **Fig. 1a**). The switching back of the backbone after each half-turn results in a structure that is a globally left-handed helix with the two strands arranged parallel to each other, but the underlying half-turns are typical right-handed B-DNA with antiparallel strand orientations.

To study the properties of switchback DNA, we first used a homodimeric sequence (strand A) that can pair with itself to form the switchback structure (**Fig. 1b, Fig. S1** and **Table S1**). The strands contain a thymine on the termini to prevent aggregation.[23] To compare switchback DNA with its canonical duplex DNA counterpart (referred to as "conventional duplex" hereafter), we designed a duplex complement (strand B). We assembled the structures and validated self-assembly using non-denaturing polyacrylamide gel electrophoresis (PAGE) (**Fig. 1b**). Since the switchback DNA (**Fig. 1b**, lane 4) migrated similar to the conventional duplex (**Fig. 1b**, lane 5), we designed a longer duplex complement by adding two Ts at the 5′ and 3′ ends, causing the duplex to migrate slower than the homodimeric switchback DNA (**Fig. 1b**, lane 6 and **Fig. S2-S3**). This result confirms that we obtained a conventional duplex with the duplex complement (with no remaining switchback structure). It is to be noted that the complement to the switchback sequence can form a homodimeric switchback structure on its own due to the sequence design (**Fig. S1**). We then constructed a heterodimeric switchback DNA from two unique strands and its corresponding duplex and validated assembly using non-denaturing PAGE (**Fig. 1c** and **Fig. S1, S4-S5**).

We then characterized the switchback DNA and the corresponding duplexes using circular dichroism (CD) spectroscopy and UV melting. The CD signature of switchback DNA was similar to that of its conventional duplex, with a positive band at 270 nm and a negative band at 250 nm, confirming that the half-turns in the switchback DNA resemble a typical B-DNA structure despite the overall left-handed nature of the switchback structure (**Fig. S6**). Thermal melting analysis showed that both the homodimeric and heterodimeric switchback structures had lower melting temperatures (Tm) compared to their duplex counterparts (**Fig. 1d and Fig. S7**), with the switchback DNA requiring at least 10 mM Mg^{2+} to be stable (**Fig. 1e**). In switchback DNA, the juxtaposition of the half-turns probably necessitates the presence of divalent ions to screen the negative charges on the backbone, similar to multi-crossover structures arranged in bundles or square lattices that also require similar Mg^{2+} concentrations to remain stable.[25,26]

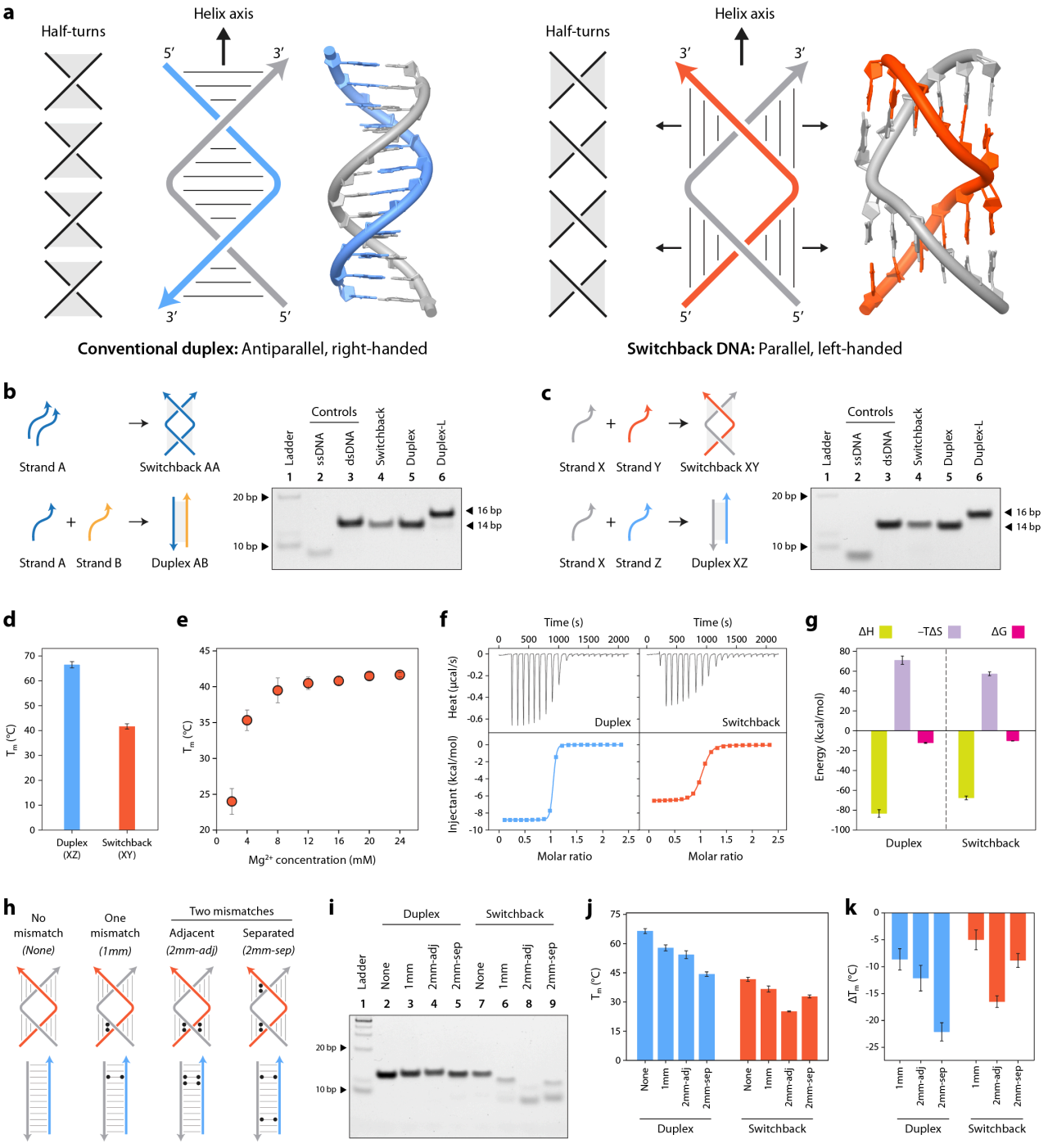

Fig. 1. ***Assembly and characterization of switchback DNA.*** (a) Schematic and model of conventional duplex and switchback DNA. Arrows denote 3′ ends of DNA strands. (b) Non-denaturing polyacrylamide gel electrophoresis (PAGE) analysis of homodimer switchback DNA. (c) Non-denaturing PAGE analysis heterodimer switchback DNA. (d) UV-thermal melting temperatures (Tm) of conventional duplex and switchback DNA. (e) Melting temperature of heterodimer switchback DNA at different Mg^{2+} concentrations. (f) Isothermal titration calorimetry (ITC) thermograms of conventional duplex and heterodimer switchback DNA. (g) Thermodynamic parameters of conventional duplex and switchback DNA. (h) Scheme of switchback DNA and conventional duplex with 1 or 2 mismatches. (i) PAGE analysis of structures with mismatches. (j-k) Melting temperatures and difference in melting temperature compared to perfectly matched sequences for conventional duplexes and switchback DNA. Data represent mean and error propagated from standard deviations of experiments performed in triplicates.

Thermodynamics of switchback DNA formation

We studied the thermodynamics of switchback DNA and conventional duplex formation using isothermal titration calorimetry (ITC) by comparing the hybridization of the two component strands in each structure (**Fig. 1f**). We measured a ΔG of −12.23 kcal/mol for the conventional duplex (with a Kd of 1.3 nM), showing that this structure was thermodynamically more stable than its switchback counterpart with a ΔG of −10.26 kcal/mol and a Kd of 30.7 nM (**Fig. 1g**). A comparison of the ΔH of the two structures (−83.33 kcal/mol for regular duplex and −67.61 kcal/mol for switchback) revealed that although the number of base pairs is the same for the two structures, the enthalpy that contributes to the stabilization of the structure is relatively less for switchback DNA (**Table S2**). Our results show that the entropic penalty for forming the duplex is higher than that for forming the switchback, which suggests that there are degrees of freedom in the switchback that don't exist in the duplex. These differences are possibly due to the disruption in the continuous base pairing and the elimination of a base stack in the middle.

Mismatch tolerance

We then investigated the contribution of the half-turn domains to the overall stability of switchback DNA by introducing mismatches in the component DNA sequences. A previous study tested the stability of such structures, but using homodimer complexes, which restricted the analysis to pairs of mismatches.[23] Here, we evaluated how the number (one or two mismatches) and the location of mismatches (one or both half-turn domains) affect the stability of the structure. To test this, we designed three variations of the heterodimeric switchback DNA: (1) a single mismatch in one domain (1mm), (2) two adjacent mismatches in one domain (2mm-adj) and (3) two mismatches spread out between the two domains of switchback DNA (one mismatch per domain) (2mm-sep) (**Fig. 1h** and **Fig. S8**). For each of these cases, we also designed duplex complements to form conventional duplexes with one or two mismatches. Non-denaturing PAGE analysis showed that the conventional duplex was not affected by the presence of one or two mismatches, as indicated by the appearance of the band similar to the control structure without any mismatches (**Fig. 1i**, lanes 2-5). For the switchback structure, presence of one mismatch did not affect the assembly. However, the formation of the switchback DNA was affected when two mismatches were introduced (**Fig. 1i**, lanes 6-9), more so when the two mismatches were adjacent to each other, indicating that both half-turn domains need to be stable to hold the full structure intact. We then measured the impact of the mismatches on the thermal stability of the structures (**Fig. 1j**). As seen with the PAGE experiment, UV melting studies also showed that the introduction of one mismatch is tolerated in a switchback structure but when two mismatches were introduced the position of the mismatch determined the stability of the structure (**Fig. 1k** and **Table S3**).

Structural preference between switchback DNA vs conventional duplex

Next, we investigated the preference of a DNA sequence to form switchback DNA or conventional duplex when presented with a switchback complement or a duplex complement. We used a longer duplex complement for these experiments to distinguish the conventional duplex from switchback DNA on non-denaturing gels. First, we studied competition between the switchback complement and the duplex complement by annealing the homodimeric switchback sequence (strand A) and its duplex complement (strand B) in different molar ratios (**Fig. 2a** and **Fig. S9**). In the absence of the duplex complement, a homodimer switchback DNA is formed. As the ratio of the duplex complement is increased, the band corresponding to the conventional duplex increases and attains maximum yield at a molar ratio of 1:1, showing that a switchback sequence prefers to form a conventional duplex in the presence of the duplex complement. Due to sequence design of switchback structures, the duplex complement can form a homodimeric switchback structure of its own, as observed with higher ratios (i.e. excess) of strand B. Normalized assembly yields showed that the strands exhibit an absolute preference for duplex (complex AB) rather than switchback DNA (complexes AA or BB), matching the expected values for maximum duplex formation at different strand ratios. We then performed a similar experiment for the heterodimeric switchback sequence (strand X) in the presence of both its switchback complement (strand Y) and duplex complement (strand Z) (**Fig. 2b** and **Fig. S10**). Again, at a ratio of 1:1:1, where 1 molar equivalent of both the switchback and duplex complements (Y and Z) were available for X, nearly all of X paired with Z to form a conventional duplex (complex XZ).

Since these observations show an absolute preference for the duplex over switchback DNA when the two competing strands are present during assembly, we then tested if the duplex complement could displace its counterpart in pre-assembled switchback DNA and convert it into a conventional duplex. We assembled homodimeric switchback DNA (complex AA) and added increasing concentrations of the duplex complement (strand B). As the concentration of the duplex complement increased, there was a concomitant increase in the amount of duplex present in the solution while the amount of switchback DNA decreased (**Fig. 2c** and **Fig. S11**). Nearly all the complexes in the solution were conventional duplexes when the duplex complement was present in 1.25 molar equivalents. Excess of the duplex complement forms a switchback complex of its own (complex BB). We observed similar results with the heterodimer switchback DNA (complex XY), with more switchback complexes converted into conventional duplexes with an increase in the concentration of the duplex complement (strand Z) (**Fig. 2d** and **Fig. S12**). Our results show that component strands have a preference towards conventional duplexes even in the presence of a switchback complement, both during and post-assembly.

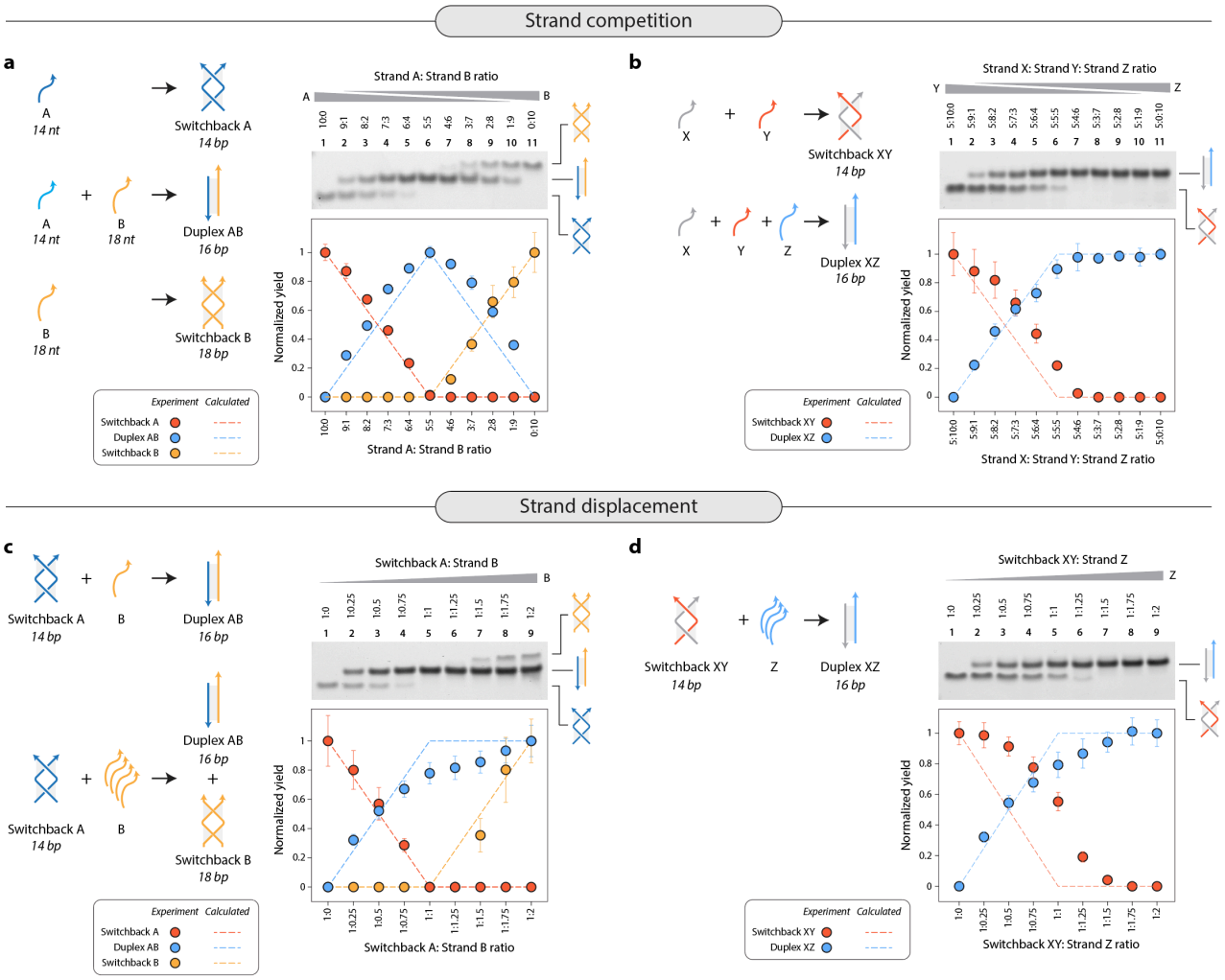

Fig. 2. ***Structural preference between conventional duplex and switchback DNA.*** (a) Assembly of homodimer switchback formed by strand A in the presence of its duplex complement B. Non-denaturing PAGE shows the formation of the homodimer switchback in the absence of its complement and increase in duplex population as the ratio of the complement in the solution increases. Excess strand B forms a homodimer switchback of its own. Quantified result of the gel bands shows decrease of switchback and increase in duplex, reaches a maximum yield at 5:5 ratio when the strands are in equal quantities. (b) Assembly of homodimer switchback formed by strands X and Y in the presence of its duplex complement Z. (c) Addition of duplex complement (strand B) to a pre-assembled homodimer switchback (complex A) causes displacement of one of the strands in the switchback, resulting in duplex formation. (d) Addition of duplex complement (strand Z) to a pre-assembled heterodimer switchback (complex XY) causes displacement of strand Y in the switchback, resulting in duplex formation (complex XZ). Data represent mean and error propagated from standard deviations of experiments performed in triplicates.

Small molecule binding to switchback DNA

Study of small molecule binding to synthetic DNA motifs and nanostructures plays a major role in the design of DNA nanostructure-based drug delivery vehicles. In that context, we analyzed the binding of two classes of small molecules (intercalators and groove binders) to switchback DNA and conventional duplex. As representative intercalators, we used ethidium bromide (EBr) and GelRed, and as representative groove binders, we used Hoechst 33258 (H33258) and 4′,6-diamidino-2-phenylindole (DAPI). These small

molecules are known to exhibit enhanced fluorescence when bound to DNA.[27–29] We incubated the homodimeric switchback DNA and its corresponding conventional duplex with different concentrations of each small molecule and measured the fluorescence signal at their characteristic emission wavelengths (**Fig. S13**). We observed that the fluorescence of small molecules upon binding to the conventional duplex was about ~1.5–2 times higher than those bound to switchback DNA in the concentration ranges we tested (**Fig. 3a-b** and **Fig. S14**). The observed difference in fluorescence enhancement is probably a consequence of fewer number of base stacks and interrupted grooves in switchback DNA compared to the regular duplex.

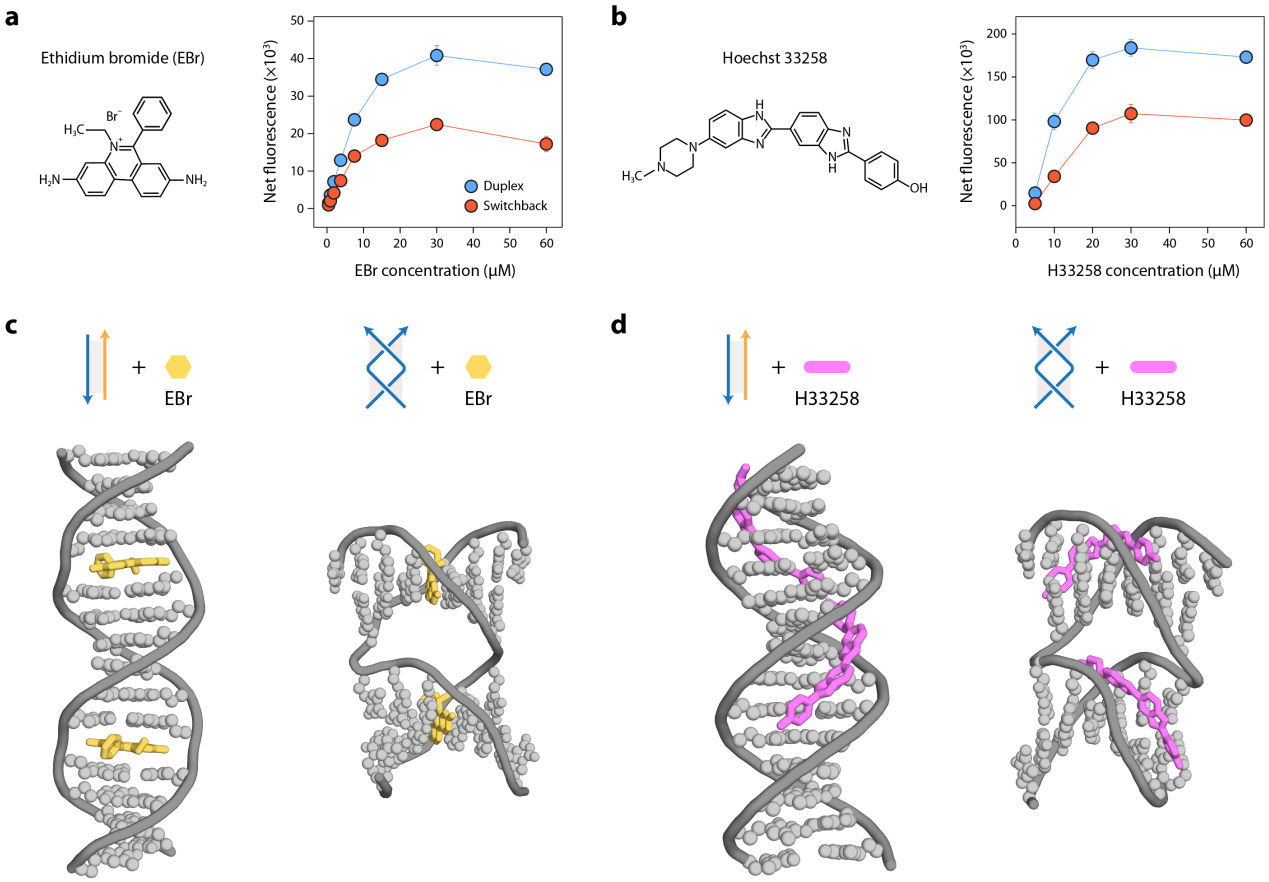

Fig. 3. ***Binding of small molecules to switchback DNA.*** (a-b) Fluorescence intensities of switchback DNA and conventional duplexes with different concentrations of EBr and Hoechst 33258, respectively. Data represent mean and error propagated from standard deviations of experiments performed in triplicates. (c-d) Molecular docking analysis of conventional duplex and switchback DNA with EBr and H33258, respectively. For EBr, two representative EBr bound intercalation sites are shown. For H33258, the bound molecules for the top two binding modes are shown.

We then performed molecular docking to obtain snapshots of how known intercalators and groove binders interact with switchback DNA compared to the conventional duplex. For the intercalator, we observed that the binding mode of EBr to the switchback DNA is similar to that of the duplex DNA. Each half-turn domain of the switchback can accommodate intercalators the same way as a duplex, without significant disruption of the structure (**Fig. 3c**). For the groove binder, we observed that the first two

binding sites with highest docking scores occurred in each half-turn domain of the switchback DNA (**Fig. 3d**). Further analysis showed that H33258 molecules prefer to bind to minor grooves but may also bind to major grooves if the minor grooves are already occupied. The continuous stretch of DNA in the duplex allows for more than one H33258 in the minor and major groove, while the switchback DNA with its two stacked half-turns is unable to accommodate more than one H33258 in either groove (**Fig. S15**).

Biostability of switchback DNA

One of the important parameters for use of DNA nanostructures in biological applications is their ability to withstand degradation by nucleases.[30] Here, we compared the biostability of switchback DNA and conventional duplexes by testing them against a variety of nucleases (**Fig. 4a**). First, we incubated both the structures with different amounts of DNase I, a commonly used endonuclease, at 37 °C for 1 hour and analyzed the nuclease treated samples using a gel-based method we established before.[31] While both structures degraded with higher amounts of DNase I, the switchback DNA showed lower degradation compared to conventional duplexes (**Fig. 4b** and **Fig. S16**). Kinetics of nuclease degradation showed that the switchback structure degraded more slowly compared to the conventional duplex when treated with DNase I (**Fig. 4c and Fig. S17**).

We then expanded our analysis to other nucleases. We incubated the switchback DNA and conventional duplex with different concentrations of T5 exonuclease (T5 exo), exonuclease III (Exo III), exonuclease V (Exo V), exonuclease VIII (Exo VIII) and micrococcal nuclease under the optimal conditions for each enzyme (**Fig. 4a-b** and **Fig. S16**). We then analyzed the degradation kinetics against these nucleases at one enzyme concentration (**Fig. 4c** and **Fig. S17**). Nucleases are known to have different activities, mechanisms, substrates, and polarities of digestion when acting on double stranded DNA. Similarly, we observed that different nucleases had varying activity levels on switchback DNA (**Fig. 4d**). In a 1 h assay, DNase I, micrococcal exonuclease and Exo V almost fully digested the switchback DNA with ~1 unit enzyme while it required ~2 units of T5 exonuclease and >10 units of Exo VIII to fully digest switchback DNA. The relative biostability of switchback DNA compared to the conventional duplex also differed for these enzymes. In DNase I and T5 Exo, the switchback DNA showed higher biostability compared to duplex whereas against Exo III, Exo VIII and micrococcal nuclease, the duplex showed higher biostability (representative data at 8 min time point is shown in **Fig. 4e**). Our results show that nuclease activity on DNA motifs can be structure dependent, with different enzymes having varying effects on DNA structures.

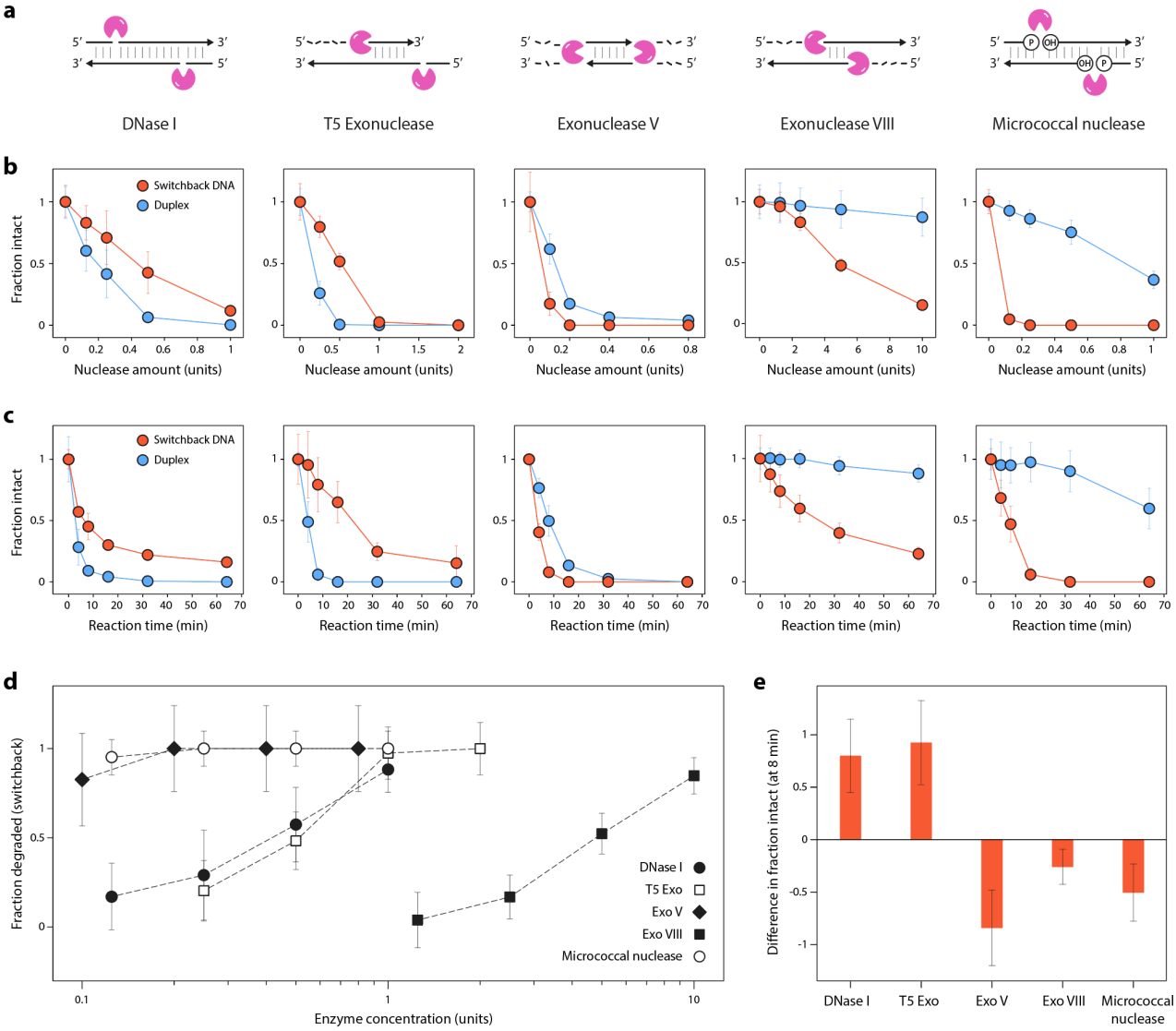

Fig. 4. ***Biostability of switchback DNA.*** (a) Known activity on duplexes of nucleases used in this study. (b) Degradation trends of switchback DNA and conventional duplex with different concentrations of each nuclease. (c) Timed analysis of switchback DNA and conventional duplex with different nucleases (DNase I: 0.75 U, T5 Exo: 1 U, Exo V: 0.5 U, Exo VIII: 10 U, micrococcal nuclease: 0.25 U). (d) Activity of different nucleases on switchback DNA. (e) Comparison of relative intact fractions of switchback DNA and conventional duplex at the 8 min time point from data shown in (c). Data represent mean and error propagated from standard deviations of experiments performed in triplicates.

Biological significance of switchback DNA

With future biological applications in mind, we tested the cell viability and immune response for switchback DNA using HeLa cells as a model cell line. We observed only a marginal reduction in cell viability after 48 hours (MTT assay) for the switchback DNA compared to the duplex, showing that the switchback DNA structure is not harmful to the cells (**Fig. 5a**). Brightfield microscopy images of the cells confirmed that switchback DNA did not interfere with cell growth when compared to cells incubated with phosphate buffered saline (PBS), 1× TAE-Mg^{2+} or untreated cells (**Fig. 5b** and **Fig. S18**). To examine the immune

response, we incubated HeLa cells with different concentrations of switchback DNA and duplex for 24 hours, isolated cellular RNA and performed RT-qPCR for three candidate markers of immune response (CXC motif chemokine ligand 8 (*CXCL-8*), chemokine (C-C motif) ligand 5 (*CCL5*) and interferon induced protein with tetratricopeptide repeats 1 (*IFIT1*). For comparison, we used 1× TAE-Mg^{2+} buffer as negative control and polyIC RNA, a synthetic stimulant known to induce immune response, as a positive control (**Fig. S18**). We observed that the expression level of *CXCL-8* was significantly lower (3- to 7-fold lower) when treated with switchback DNA than when treated with duplex across the concentration range of 100-1000 nM of DNA (**Fig. 5c**). We did not observe substantial differences in the levels of the other two markers between switchback DNA and duplex (**Fig. 5c**), whereas polyIC treatment induced *CCL5* expression (**Fig. S18**). Overall, our results show that switchback DNA induced lower expression of immune response markers compared to duplex DNA or polyIC in HeLa cells for the markers tested here. These findings suggest that switchback DNA could potentially be a low-immunogenic alternative to duplex-based nanostructures for biological applications.

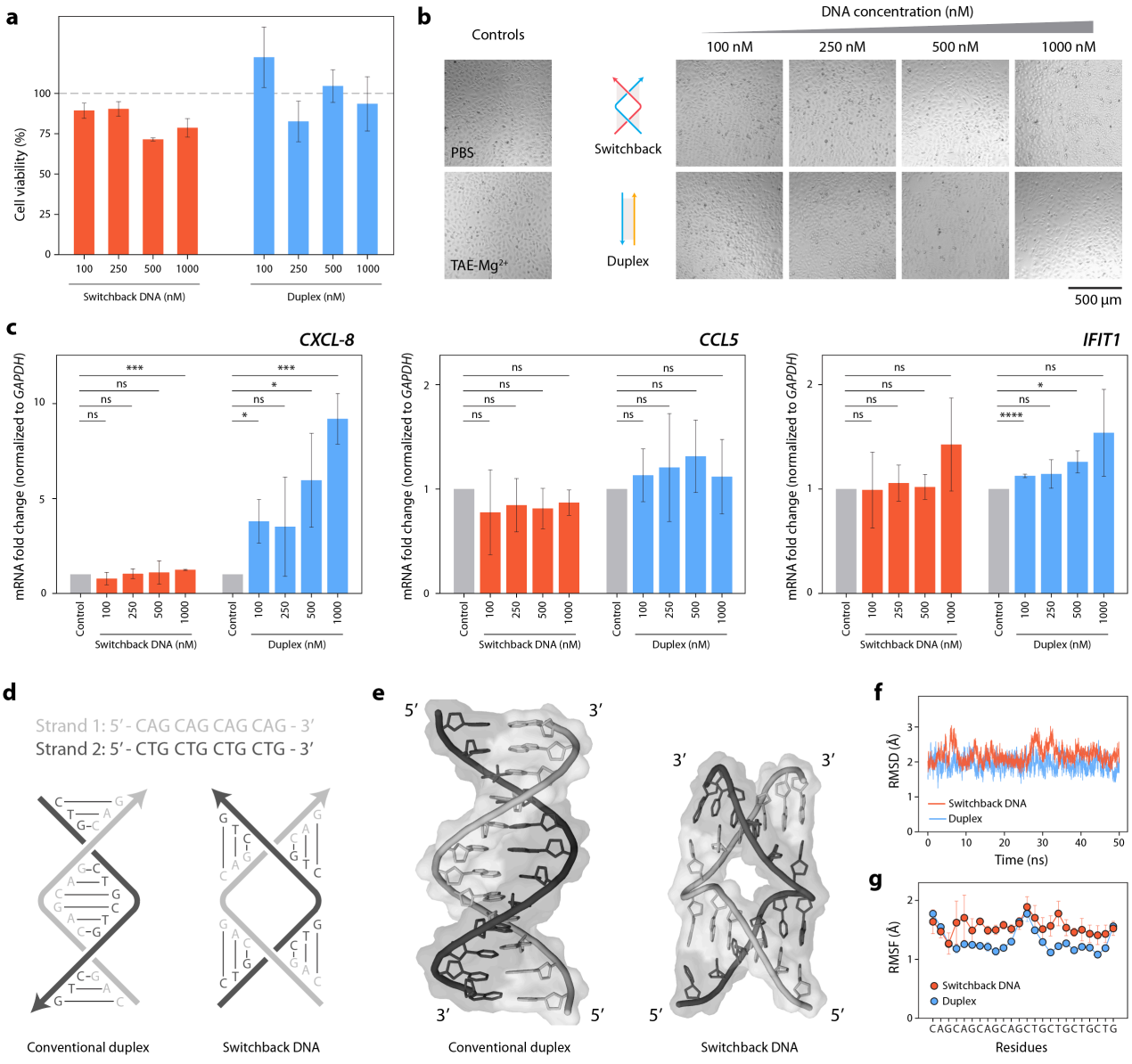

Fig. 5. *Biological studies.* (a) Viability of cells treated with switchback DNA and conventional duplex at different DNA concentrations. Data is normalized to viability of cells treated with 1× TAE-Mg^{2+} (gray line). (b) Brightfield microscopy images of cells treated with different concentrations of switchback DNA and conventional duplex. (c) RT-qPCR analysis of immune response markers in cells. Data represent mean and standard deviation from three biological replicates. Unpaired two-tailed *t*-test was used to compare switchback DNA and duplex DNA treatments to controls, ns – not significant, $*P < 0.05$, $***P < 0.001$, $****P < 0.0001$. (d) A pair of repeat sequences that can form a conventional duplex or switchback DNA. (e) Simulated structures of repeat sequences forming switchback DNA or conventional duplex. (f) Root mean square deviation (RMSD) of the duplex and switchback as a function of time. (g) Root mean square fluctuations (RMSF) of residues in the duplex and switchback. Error bars show the standard deviation from three replicates.

We next considered the biological significance of sequences that can form switchback DNA and hypothesize that switchback DNA could be a potential alternate structure for sequences involved in repeat expansion diseases. Expansion of short tandem repeats (stretches of 2-12-bp-long repeating tracts of DNA) found in both coding and non-coding regions of the genome causes over 50 neurological, neuromuscular and neurodegenerative diseases.[32] Many of these repeat sequences have been shown to form non-canonical DNA structures such as hairpins [e.g. spinocerebellar ataxia type 2, CAGn],[33] G-quadruplexes [e.g. *C9orf72* amyotrophic lateral sclerosis-frontotemporal dementia, (GGGGCC)•(GGCCCC)],[34] triplexes [e.g. Friedreich's ataxia, (GAA•TTC)],[35] Z-DNA [e.g. myotonic dystrophy type 2, CCTG•CAGG][36] and slipped DNA junctions [e.g. myotonic dystrophy type 1, (CTG)•(CAG) and fragile X syndrome (CGG)•(CCG)].[37] These alternate structures can influence DNA repeat instability, transcription, translation, and protein binding.[38] We screened various sequences involved in repeat expansion diseases and observed that in some cases, a given sequence could have the same switchback complement and duplex complement (**Fig. S19**). That is, a pair of sense and antisense strands containing tandem repeat sequences could form either the switchback DNA or a conventional duplex (**Fig. 5d**).

To study the relevance of switchback DNA in tandem repeat sequences, we chose the trinucleotide repeat $(CAG)_4$ and its complement $(CTG)_4$ associated with Huntington disease, various spinocerebellar ataxias, myotonic dystrophy type 1, and Fuchs endothelial corneal dystrophy.[39] We performed molecular dynamics (MD) simulations to study the conformational dynamics of the two structures formed by these same pair of strands (**Fig. 5d-e**). Our simulations indicate that once formed, the overall structure of the switchback DNA is well tolerated by the repeat sequences, as indicated by only a marginally higher root mean square deviation (RMSD) throughout the simulations compared to the duplex (**Fig. 5f**). Next, we calculated the fluctuations of the nucleotides in the two structures. Higher fluctuation is suggestive of weaker interactions leading to local instability. We observed that the fluctuations of the two structures are higher on the terminal nucleotides, which is expected. However, switchback DNA shows consistently higher fluctuations compared to the duplex, which suggests localized regions where the structure is more likely to unfold compared to the duplex (**Fig. 5g**). Based on sequence analysis of repeat expansion diseases and

the MD simulations, we hypothesize that certain repeat sequences allow both switchback complementarity and conventional complementarity when the sequences contain di, tri, tetra and hexanucleotide repeat sequences (**Fig. S19**). In previous works, synthetic DNA motifs such as PX DNA have been implied to have biological relevance and structure-specific binding of proteins.[40] Similarly, the switchback DNA structure could be a transient or intermediate structure in biological or disease processes.

Conclusions

In this work, we provide a detailed characterization of the structural and dynamic properties of switchback DNA. Our results show that while switchback DNA is stable, it requires higher Mg^{2+} levels compared to a conventional duplex, but within the range of most DNA motifs and nanostructures. By introducing mutations in the sequence, we show domain-dependent stability of the switchback DNA, information that is useful in higher-order nanostructure design. The structural preference of component strands to form either switchback DNA or conventional duplex could be used in controlling sub-populations within a mixture[41] and in toehold-less strand displacement.[42] This strategy works on the structure-specific affinity of a set of DNA strands (rather than the typical sequence-based affinity) and will allow for multiple displacement cascades as the displaced strand has a sequence distinct from the complement. Our observation that nuclease resistance levels vary for different structures and that thermal stability (or instability) does not always correspond to biostability is consistent with our earlier work with PX DNA.[17] Our study on small molecule binding provides insight into design-based loading of small molecules on DNA nanostructures, and these results that hold significance in studying the drug loading efficiencies of DNA nanostructure-based drug carriers. Our biological studies show that switchback DNA has a marginal effect on cell viability and induces lower immune response than a conventional duplex when selected markers were tested in the HeLa cell line. Specifically, switchback DNA exhibited significantly lower expression of *CXCL-8* compared to duplex. *CXCL-8* has been known to promote tumoral angiogenesis and reducing the adverse effects of *CXCL-8* signaling may be beneficial in cancer treatment.[43] These results could therefore help inform the design of DNA-based carriers and nanodevices that target the tumor microenvironment. Combined, these results provide important information for potential use of the switchback structure in biology and medicine.

In addition to the assembly and characterization of switchback DNA, we suggest a biological relevance for the molecule. The sequence requirement for formation of the switchback DNA structure is satisfied by short tandem repeat sequences that are present widely in the eukaryotic genome and known to form alternate structures such as hairpins,[33] G-quadruplexes,[34] triplexes[35] and minidumbbells.[44] While G-quadruplexes are found only in G-rich sequences[34] and minidumbbells are seen in pyrimidine-rich repeat sequences,[44] the switchback structure does not have such base composition requirements. Minidumbells[44] and foldback DNA intercoil[45] that occur in nature require high concentrations of divalent ions to form,

indicating that the requirement of higher Mg^{2+} concentrations for switchback DNA does not reduce its biological relevance. Non-B DNA structures stabilized by Ca^{2+} also occur in dinucleotide $(TG/AC)_n$ repeats, which suggests the possible involvement of divalent ion-stabilized DNA secondary structures in various dynamic processes at the chromosomal level.[46] While MD simulations show that repeat sequences can remain stable when folded into switchback form, it remains to be seen whether these sequences adopt the structure under physiological or pathological conditions. As an alternative DNA conformation that still uses the canonical Watson-Crick-Franklin hydrogen bonding, the switchback structure gains relevance because it allows the expansion of the scope of sequence complementarity. That is, for any given sequence it is possible to dictate a switchback complement sequence just as readily as the regular complementary sequence.

In DNA nanotechnology, switchback DNA structure can be combined with sticky ends to create double-crossover-like structures that are used in 3D assemblies.[24] Larger constructs based on switchback DNA are possible but may require chemical functionalization (such as 3′-3′ or 5′-5′ linkages) to allow for strand connectivity since the two strands in the structure are parallel. The left-handedness of switchback DNA can be an advantage in some cases. In topological studies of catenanes and knots, structures constructed using conventional right-handed B-DNA duplexes have negative nodes,[47] and require the use of left-handed Z-DNA or L-DNA to produce a positive node. Incorporation of Z-DNA requires specific sequences and ionic conditions while L-DNA requires expensive chemical synthesis. In such cases, use of a switchback structure will provide a positive node due to its left-handedness. Further, switchback complementarity could be used to connect DNA motifs as an alternate for sticky ended cohesion, such as with bubble-bubble cohesion[48] or paranemic cohesion.[49] The requirement of Mg^{2+} to form stable switchback DNA could also be useful in ion-dependent assembly of DNA nanostructures, similar to DNA nanostructures constructed through loop-loop interactions at high Mg^{2+} concentrations.[41] Overall, our study provides further understanding of the switchback DNA structure, with utility in nanotechnology to fold DNA into stable and functional structures, and biological relevance in repeat disorders combined with biostability and biological feasibility that allows its use in several different applications.

Data availability

The data that support the findings of this study are available within the paper and its Supplementary Information. Any other data are available from the corresponding author on request.

Competing interests

The authors have no competing interests.

Author contributions

B.R.M. and A.R.C. designed experiments. B.R.M. performed ITC, CD, and UV melting experiments and analyzed the corresponding data. B.R.M., H.T., and A.R. performed gel electrophoresis for assembly and characterization of DNA complexes. B.R.M. and A.R. performed fluorescence spectroscopy experiments and analyzed the corresponding data. H.T., A.R. and A.R.C. performed gel electrophoresis for biostability experiments. B.R.M. and A.R.C. analyzed gel electrophoresis results. H.Z. and S.V. performed molecular dynamics simulations and molecular docking and analyzed the corresponding data. J.M.L. performed cell studies. J.M.L and K.R. analyzed the corresponding data. A.R.C. conceived and supervised the project and visualized the data. B.R.M. and A.R.C. wrote the manuscript with contributions from S.V. and K.R.

Acknowledgments

Research reported in this publication was supported by the National Institutes of Health (NIH) through National Institute of General Medical Sciences (NIGMS) under award number R35GM150672 to A.R.C., State University of New York institutional start-up funds to K.R. and NSF SAGES grant to S.V. J.M.L was supported by a Myotonic Dystrophy Foundation Postdoctoral Fellowship. We thank Jibin Abraham Punnoose and Ken Halvorsen for helpful discussions and comments on the paper.

References

1. Xavier, P. L. & Chandrasekaran, A. R. DNA-based construction at the nanoscale: emerging trends and applications. *Nanotechnology* **29**, 062001 (2018).
2. Fu, T. J. & Seeman, N. C. DNA double-crossover molecules. *Biochemistry* **32**, 3211–3220 (1993).
3. LaBean, T. H. *et al.* Construction, Analysis, Ligation, and Self-Assembly of DNA Triple Crossover Complexes. *J. Am. Chem. Soc.* **122**, 1848–1860 (2000).
4. Shen, Z., Yan, H., Wang, T. & Seeman, N. C. Paranemic Crossover DNA: A Generalized Holliday Structure with Applications in Nanotechnology. *J. Am. Chem. Soc.* **126**, 1666–1674 (2004).
5. He, Y., Chen, Y., Liu, H., Ribbe, A. E. & Mao, C. Self-Assembly of Hexagonal DNA Two-Dimensional (2D) Arrays. *J. Am. Chem. Soc.* **127**, 12202–12203 (2005).
6. He, Y., Tian, Y., Ribbe, A. E. & Mao, C. Highly Connected Two-Dimensional Crystals of DNA Six-Point-Stars. *J. Am. Chem. Soc.* **128**, 15978–15979 (2006).
7. He, Y. *et al.* Hierarchical self-assembly of DNA into symmetric supramolecular polyhedra. *Nature* **452**, 198–201 (2008).
8. Stewart, J. M., Geary, C. & Franco, E. Design and Characterization of RNA Nanotubes. *ACS Nano* **13**, 5214–5221 (2019).

9. Liu, D., Park, S. H., Reif, J. H. & LaBean, T. H. DNA nanotubes self-assembled from triple-crossover tiles as templates for conductive nanowires. *Proceedings of the National Academy of Sciences* **101**, 717–722 (2004).
10. Shen, W. *et al.* The study of the paranemic crossover (PX) motif in the context of self-assembly of DNA 2D crystals. *Org. Biomol. Chem.* **14**, 7187–7190 (2016).
11. Hong, F. *et al.* Layered-Crossover Tiles with Precisely Tunable Angles for 2D and 3D DNA Crystal Engineering. *J. Am. Chem. Soc.* **140**, 14670–14676 (2018).
12. Wintersinger, C. M. *et al.* Multi-micron crisscross structures grown from DNA-origami slats. *Nat. Nanotechnol.* **18**, 281–289 (2023).
13. Ke, Y. *et al.* DNA brick crystals with prescribed depths. *Nature Chem* **6**, 994–1002 (2014).
14. Marras, A. E., Zhou, L., Su, H.-J. & Castro, C. E. Programmable motion of DNA origami mechanisms. *PNAS* **112**, 713–718 (2015).
15. Chandrasekaran, A. R., Levchenko, O., Patel, D. S., MacIsaac, M. & Halvorsen, K. Addressable configurations of DNA nanostructures for rewritable memory. *Nucleic Acids Res* **45**, 11459–11465 (2017).
16. Ohayon, Y. P. *et al.* Covalent Linkage of One-Dimensional DNA Arrays Bonded by Paranemic Cohesion. *ACS Nano* **9**, 10304–10312 (2015).
17. Chandrasekaran, A. R. *et al.* Exceptional Nuclease Resistance of Paranemic Crossover (PX) DNA and Crossover-Dependent Biostability of DNA Motifs. *J. Am. Chem. Soc.* **142**, 6814–6821 (2020).
18. Wunnicke, D., Ding, P., Yang, H., Seela, F. & Steinhoff, H.-J. DNA with Parallel Strand Orientation: A Nanometer Distance Study with Spin Labels in the Watson–Crick and the Reverse Watson–Crick Double Helix. *J. Phys. Chem. B* **119**, 13593–13599 (2015).
19. Kulkarni, P., Datta, D. & Ganesh, K. N. Gemdimethyl Peptide Nucleic Acids (α/β/γ-gdm-PNA): E/Z-Rotamers Influence the Selectivity in the Formation of Parallel/Antiparallel gdm-PNA:DNA/RNA Duplexes. *ACS Omega* **7**, 40558–40568 (2022).
20. van de Sande, J. H. *et al.* Parallel Stranded DNA. *Science* **241**, 551–557 (1988).
21. Mao, C., Sun, W., Shen, Z. & Seeman, N. C. A nanomechanical device based on the B–Z transition of DNA. *Nature* **397**, 144–146 (1999).
22. Lin, C. *et al.* Mirror Image DNA Nanostructures for Chiral Supramolecular Assemblies. *Nano Lett.* **9**, 433–436 (2009).
23. Tian, C. *et al.* Artificial, Parallel, Left-Handed DNA Helices. *J. Am. Chem. Soc.* **134**, 20273–20275 (2012).

24. Zhang, C. *et al.* Engineering DNA Crystals toward Studying DNA–Guest Molecule Interactions. *J. Am. Chem. Soc.* **145**, 4853–4859 (2023).
25. Ke, Y. *et al.* Multilayer DNA Origami Packed on a Square Lattice. *J. Am. Chem. Soc.* **131**, 15903–15908 (2009).
26. Zhang, Y., Yang, D., Wang, P. & Ke, Y. Building Large DNA Bundles via Controlled Hierarchical Assembly of DNA Tubes. *ACS Nano* **17**, 10486–10495 (2023).
27. Olmsted, J. I. & Kearns, D. R. Mechanism of ethidium bromide fluorescence enhancement on binding to nucleic acids. *Biochemistry* **16**, 3647–3654 (1977).
28. Loontiens, F. G., Regenfuss, P., Zechel, A., Dumortier, L. & Clegg, R. M. Binding characteristics of Hoechst 33258 with calf thymus DNA, poly[d(A-T)] and d(CCGGAATTCCGG): multiple stoichiometries and determination of tight binding with a wide spectrum of site affinities. *Biochemistry* **29**, 9029–9039 (1990).
29. Sapia, R. J., Campbell, C., Reed, A. J., Tsvetkov, V. B. & Gerasimova, Y. V. Interaction of GelRed™ with single-stranded DNA oligonucleotides: Preferential binding to thymine-rich sequences. *Dyes and Pigments* **188**, 109209 (2021).
30. Chandrasekaran, A. R. Nuclease resistance of DNA nanostructures. *Nature Reviews Chemistry* **5**, 225–239 (2021).
31. Chandrasekaran, A. R. & Halvorsen, K. Nuclease degradation analysis of DNA nanostructures using gel electrophoresis. *Current Protocols in Nucleic Acid Chemistry* **82**, e115 (2020).
32. Sznajder, Ł. J. & Swanson, M. S. Short Tandem Repeat Expansions and RNA-Mediated Pathogenesis in Myotonic Dystrophy. *International Journal of Molecular Sciences* **20**, 3365 (2019).
33. Sobczak, K. & Krzyzosiak, W. J. CAG Repeats Containing CAA Interruptions Form Branched Hairpin Structures in Spinocerebellar Ataxia Type 2 Transcripts*. *Journal of Biological Chemistry* **280**, 3898–3910 (2005).
34. Zamiri, B., Mirceta, M., Bomsztyk, K., Macgregor, R. B., Jr. & Pearson, C. E. Quadruplex formation by both G-rich and C-rich DNA strands of the C9orf72 (GGGGCC)8•(GGCCCC)8 repeat: effect of CpG methylation. *Nucleic Acids Research* **43**, 10055–10064 (2015).
35. Sakamoto, N. *et al.* Sticky DNA: Self-Association Properties of Long GAA·TTC Repeats in R·R·Y Triplex Structures from Friedreich's Ataxia. *Molecular Cell* **3**, 465–475 (1999).
36. Edwards, S. F., Sirito, M., Krahe, R. & Sinden, R. R. A Z-DNA sequence reduces slipped-strand structure formation in the myotonic dystrophy type 2 (CCTG)·(CAGG) repeat. *Proceedings of the National Academy of Sciences* **106**, 3270–3275 (2009).

37. Pearson, C. E. & Sinden, R. R. Alternative Structures in Duplex DNA Formed within the Trinucleotide Repeats of the Myotonic Dystrophy and Fragile X Loci. *Biochemistry* **35**, 5041–5053 (1996).
38. Malik, I., Kelley, C. P., Wang, E. T. & Todd, P. K. Molecular mechanisms underlying nucleotide repeat expansion disorders. *Nat Rev Mol Cell Biol* **22**, 589–607 (2021).
39. Paulson, H. Chapter 9 - Repeat expansion diseases. in *Handbook of Clinical Neurology* (eds. Geschwind, D. H., Paulson, H. L. & Klein, C.) vol. 147 105–123 (Elsevier, 2018).
40. Kizer, M. *et al.* Complex between a Multicrossover DNA Nanostructure, PX-DNA, and T7 Endonuclease I. *Biochemistry* **58**, 1332–1342 (2019).
41. Zheng, M. *et al.* Kinetic DNA Self-Assembly: Simultaneously Co-folding Complementary DNA Strands into Identical Nanostructures. *J. Am. Chem. Soc.* **143**, 20363–20367 (2021).
42. Li, Y., Zhang, C., Tian, C. & Mao, C. A nanomotor involves a metastable, left-handed DNA duplex. *Org. Biomol. Chem.* **12**, 2543–2546 (2014).
43. Waugh, D. J. J. & Wilson, C. The Interleukin-8 Pathway in Cancer. *Clinical Cancer Research* **14**, 6735–6741 (2008).
44. Liu, Y. *et al.* Structures and conformational dynamics of DNA minidumbbells in pyrimidine-rich repeats associated with neurodegenerative diseases. *Computational and Structural Biotechnology Journal* **21**, 1584–1592 (2023).
45. Kim, B.-D. Foldback Intercoil DNA and the Mechanism of DNA Transposition. *Genomics Inform* **12**, 80–86 (2014).
46. Dobi, A. & v. Agoston, D. Submillimolar levels of calcium regulates DNA structure at the dinucleotide repeat (TG/AC)n. *Proceedings of the National Academy of Sciences* **95**, 5981–5986 (1998).
47. Ciengshin, T., Sha, R. & Seeman, N. C. Automatic Molecular Weaving Prototyped by Using Single-Stranded DNA. *Angewandte Chemie International Edition* **50**, 4419–4422 (2011).
48. Qian, H., Yu, J., Wang, P., Dong, Q.-F. & Mao, C. DNA cohesion through bubble–bubble recognition. *Chem. Commun.* **48**, 12216–12218 (2012).
49. Zhang, X., Yan, H., Shen, Z. & Seeman, N. C. Paranemic Cohesion of Topologically-Closed DNA Molecules. *J. Am. Chem. Soc.* **124**, 12940–12941 (2002).